

σ -donating MO's are not expected to be influenced by the conjugation mechanism. For the substituents with α -carbon or nitrogen, the $e_g(\pi^*)$ level is apparently far from empty or filled 2p orbitals of the substituents, but the filled $e_g(\pi)$ orbitals are relatively close to the filled 2p orbitals. Therefore, the filled $e_g(\pi)$ orbitals are stabilized by conjugation with substituent 2p orbitals that may lie at higher energy than $e_g(\pi)$. For the chlorine substituents, the conjugation of filled 3p orbitals and $e_g(\pi^*)$ should also be taken into consideration. In the case of Pc, the substituents are replaced by hydrogens, which do not permit such conjugation because suitable p orbitals are not available. Thus, the conjugation mechanism is expected to modulate Π in diverse ways depending upon the type of the substituents.

As described above, the inductive mechanism causes the decrease of both Σ and Π with $\Sigma\sigma$. Equation 4 implies that the difference between Π and Σ is δ . The unsystematic variation of δ with $\Sigma\sigma$ in Table I is thought to be due in part by the conjugation that modifies only Π diversely. Furthermore, the delicate difference of the effective populations of 3d, 4s, and 4p orbitals must be amplified to give an apparently irregular distribution of data points in Figure 2. We succeeded in extracting information about the σ - and π -bonding properties of the phthalocyaninato ligands from such irregular data.

Porphyrin Complexes. Several tetracoordinate planar porphyrin complexes are included in Table I and Figure 3, for comparison: (octaethylporphyrinato)iron(II), Fe(OEP),²⁸ (tetraphenylporphyrinato)iron(II), Fe(TPP),²⁷ and (octamethyltetrabenzoporphyrinato)iron(II), Fe(OMTBP).²⁹ The basicity is thought to decrease in the order Pc > OEP > TPP > OMTBP, on the basis of redox potentials of the porphyrins and other experimental results. The calculated values of bonding parameters also decrease in the same order: decreasing the porphyrin basicity places less electron density on the iron. Reasonable orders of bonding parameters were obtained on the basis of the assumption that the ground-state configurations in these complexes are the same as in the (phthalocyaninato)iron(II) complexes. Although some

studies suggest^{30,33} a ground state for (porphyrinato)iron(II) different from that for (phthalocyaninato)iron(II), the present study favors the same configuration in these two systems.

The values of a and b in eq 5 are rather ambiguous, as stated above. Detailed considerations proved, however, that b should be larger than 0.421 in order to give a larger Σ for Pc than for other substituted phthalocyanines, a should be smaller than 1.775 in order to give a smaller Π for OMTBP than for all phthalocyanines, and any pair of a and b satisfying $0.421 < b < a < 1.775$ does not change the orders of Σ 's and Π 's in Table I and Figure 3. Our determination of the bonding parameters is believed to be adequate.

Conclusion

Two kinds of bonding parameters, Σ and Π , were introduced for substituted phthalocyanines to interpret Mössbauer parameters, δ and ΔE_Q , of tetracoordinate (phthalocyaninato)iron(II) complexes in connection with the bonding characteristics of the macrocyclic ligands. They represent σ - and π -bonding properties, respectively, and are defined to be larger when more electron density is placed on the iron. The orders of calculated Σ and Π are in a good correlation with the sum of the Hemmett σ constants, $\Sigma\sigma$, of the substituents.

Several tetracoordinate (porphyrinato)iron(II) complexes were treated in the same manner. The bonding parameters, Σ and Π , are found to decrease in the decreasing order of the basicity of the porphyrinato ligands. The present study favors the same ground-state configuration for (porphyrinato)iron(II) as for (phthalocyaninato)iron(II).

In sum, the apparently irregular variation of δ and ΔE_Q of tetracoordinate iron(II) complexes is interpreted systematically. A study of (phthalocyaninato)iron(II) complexes with electron-releasing substituents is in progress.

Acknowledgment. This work was partially supported by a Grant-in-Aid for Scientific Research from the Ministry of Education, No. 61540456.

Contribution from the Department of Chemistry,
University of Ottawa, Ottawa, Ontario, Canada K1N 6N5

Time-Resolved FTIR Study of the Adsorption and Reaction of Co(CO)₃NO on Alumina

J. L. Roustan,* Y. Lijour, and B. A. Morrow*

Received October 27, 1986

Deposition of Co(CO)₃(NO) gas on alumina preactivated at 450 °C occurs readily at room temperature to yield two mononitrosyl species with $\nu(\text{NO})$ at 1795 and 1700 cm⁻¹, respectively. Time-resolved FTIR spectroscopy shows that within minutes these initial species start to react and yield more than one type of surface isocyanate, (NCO)_s, as well as other surface nitrosyl species. Without evacuation of the reactant, (NCO)_s formation proceeds slowly over a 7-day period, accompanied by the appearance of bands due to a surface dinitrosyl with $\nu(\text{NO})$ at 1880 and 1800 cm⁻¹, and CO is released to the gas phase. The formation of (NCO)_s is greatly accelerated under vacuum, but the predominant surface nitrosyl generated is now a mononitrosyl with $\nu(\text{NO})$ at 1830 cm⁻¹. The latter is easily converted into the 1880/1800-cm⁻¹ dinitrosyl species in the presence of CO. Codeposition of Co(CO)₃(NO) with an excess of either CO or NO very efficiently inhibits the formation of isocyanates. In the presence of CO, the 1795- and 1700-cm⁻¹ species show no sign of significant decomposition even after 4 days. Under NO, however, they are converted into the 1880/1800-cm⁻¹ dinitrosyl species.

Introduction

NO gas has frequently been used as a chemical probe to assess the nature of metallic sites present on a surface following deposition of a suitable metallic precursor (see for example ref 1). An alternative and complementary approach is to deposit a metallic element with the NO probe already attached to it. For example, Mo(CH₃CN)₄(NO)₂⁺BF₄⁻ deposited on alumina has provided a

model for NO reactions on Mo/Al₂O₃ surfaces.²

Although there have been many studies of the deposition of metal carbonyls on various surfaces,³ including Co₂(CO)₈ on alumina (see ref 4 and 5 and references therein), the use of

(1) (a) Topsoe, N. Y.; Topsoe, H. *J. Catal.* **1982**, *75*, 354. (b) King, D. L.; Perri, J. B. *J. Catal.* **1983**, *105*, 1689. (c) Kung, M. C.; Kung, H. *H. Catal. Rev.—Sci. Eng.* **1985**, *27*, 425.

(2) Rosen, R. P.; Segawa, K.; Millan, W. S.; Hall, W. K. *J. Catal.* **1984**, *90*, 368.

(3) Basset, J. M.; Choplin, A. *J. Mol. Catal.* **1983**, *21*, 95.

(4) Schneider, R. L.; Howe, R. F.; Watters, K. L. *Inorg. Chem.* **1984**, *23*, 4593.

(5) Iwasawa, Y.; Yamada, M.; Sato, Y.; Kuroda, H. *J. Mol. Catal.* **1984**, *23*, 95.

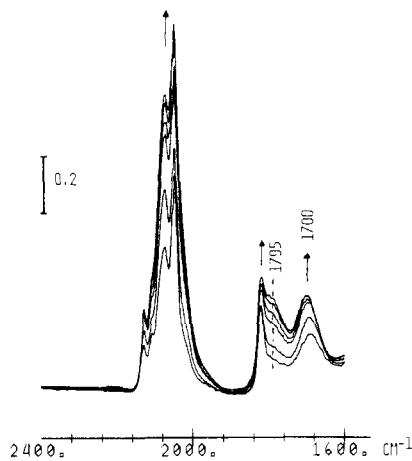


Figure 1. Infrared spectra observed during the initial deposition of $\text{Co}(\text{CO})_3\text{NO}$ on alumina after (from bottom to top) 5, 10, 20, 30, 50, and 70 s (gas phase not subtracted).

carbonyl-nitrosyl derivatives has been largely overlooked. In this paper, the first of a series concerning the interactions of nitrosyl complexes with a surface, we report our results regarding the deposition of $\text{Co}(\text{CO})_3(\text{NO})$ on alumina preactivated at 450°C . After completion of this work, the same compound has been reported very recently to interact with a zeolite to yield catalytically active surfaces in the Fischer-Tropsch reaction.⁶

To our knowledge, the work presented here is the first attempt to delineate the intricate nature of the chemical events occurring during and after deposition, when a nitrosyl-carbonyl transition-metal complex is allowed to interact with a refractory oxide at room temperature. This study has been greatly facilitated by the use of time-resolved FTIR spectroscopy.

Experimental Section

$\text{Co}(\text{CO})_3(\text{NO})$ was purchased from Strem Chemical Inc. All experiments were carried out with 20 mg cm^{-2} disks of Degussa Alumin Oxid C (mainly a γ -alumina having a BET surface area of $105\text{ m}^2\text{ g}^{-1}$), which were pressed in a stainless steel die at 10^7 Pa . The disk was mounted in a standard infrared cell,⁷ and it was activated under vacuum at 450°C for 1 h prior to admission of 1 Torr of $\text{Co}(\text{CO})_3\text{NO}$. In light of the high volatility of $\text{Co}(\text{CO})_3(\text{NO})$ at room temperature, the deposition step is exceedingly simple. A flask containing the reagent in equilibrium with its vapor is connected to a chamber that is attached to the cell through a side arm. The cell and the chamber, isolated from the flask, are pumped under vacuum and then isolated from the vacuum line. $\text{Co}(\text{CO})_3(\text{NO})$ gas is allowed to expand in the chamber, isolated from the cell, and subsequently from the chamber now isolated from the flask into the cell. The total deposition of the initial load of $\text{Co}(\text{CO})_3(\text{NO})$ on the disk corresponds to $160\text{ }\mu\text{mol g}^{-1}$ of alumina or about 1.0% cobalt. Half this quantity was used in some experiments, and no spectral differences were noted beyond reduced band intensities.

All spectra were recorded with a Bomem DA3-02 FTIR spectrometer at a resolution of 4.0 cm^{-1} , and all reported spectra were plotted without additional smoothing. Generally 100 scans were coadded (total scan time 30 s), although during time-resolved studies single scans at 0.5-s intervals could be acquired. Gas-phase analyses were carried out with the FTIR instrument and a quadrupole mass spectrometer, or with a high-resolution mass spectrometer in order to distinguish between species of the same mass number (e.g. N_2 and CO). Coadsorption experiments with excess CO or NO were carried out by admitting a mixture of 1 Torr of $\text{Co}(\text{CO})_3\text{NO}$ and about 30 Torr of CO or NO.

Results

Liquid $\text{Co}(\text{CO})_3\text{NO}$ is deep brown, and in the gas phase (vapor pressure ~ 80 Torr at 25°C) it is pale yellow. Upon admission of 1 Torr to the infrared cell the alumina disk immediately turned yellow, and over a matter of several minutes this progressively turned to brown as the yellow color of the gas disappeared. Gaseous $\text{Co}(\text{CO})_3\text{NO}$ has two sharp $\nu(\text{CO})$ hands at 2104 and 2043 cm^{-1} and a sharp $\nu(\text{NO})$ band at 1817 cm^{-1} with relative

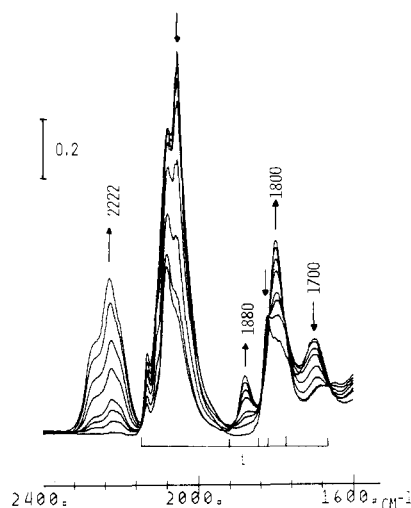


Figure 2. Spectra recorded 4 min, 17 min, 45 min, 6 h, 18 h, 42 h, and 84 h after admission of $\text{Co}(\text{CO})_3\text{NO}$ onto Al_2O_3 (gas phase not subtracted). Arrows indicate increasing or decreasing intensity changes.

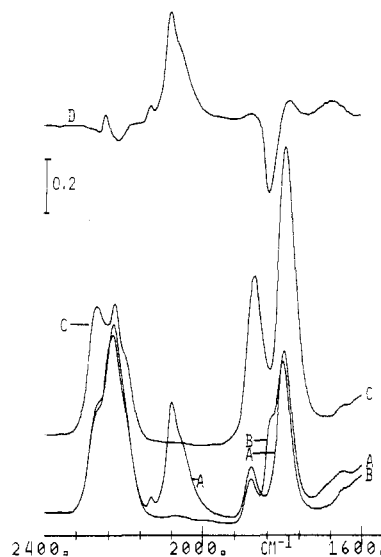


Figure 3. Admission of $\text{Co}(\text{CO})_3\text{NO}$ onto Al_2O_3 : (A) spectrum 7 days after admission; (B) spectrum after evacuation for 12 h; (C) spectrum after addition of 30 Torr of NO to (B); (D) difference spectrum (A) - (B) showing the spectral changes on evacuation.

intensities of about 1:3:2, respectively. About 85% of the admitted vapor adsorbed on the alumina within 15 min, and the remainder slowly disappeared over the next 40 h if the cell was not evacuated.

Figure 1 shows the spectral changes from 2400 to 1600 cm^{-1} that were observed during the first 1 min of adsorption (no spectral changes were observed in other spectral regions). In addition to the bands due to gaseous $\text{Co}(\text{CO})_3\text{NO}$ new broader bands appeared and gradually intensified at 1700, 1795, 2050, 2070, 2105, and 2128 cm^{-1} . As will be demonstrated later, the 1700/1795- cm^{-1} bands are due to $\nu(\text{NO})$ modes (and their relative intensities varied during this initial adsorption) whereas the bands above 2000 cm^{-1} are due to $\nu(\text{CO})$ modes.

Figures 2 and 3 show the spectral changes observed from 4 min up to 7 days of adsorption. Beyond 4 min of adsorption the CO bands and the 1700-cm^{-1} band decreased in intensity (in addition to the bands due to gas-phase $\text{Co}(\text{CO})_3\text{NO}$), and new strong bands started to grow at 2272, 2222, 2200, 1880, and 1800 cm^{-1} , along with several weak broad bands between 1585 and 1220 cm^{-1} . There were six isosbestic points, which are indicated by "i" in Figure 2.

It will be shown below that the bands at 2272, 2222, and 2200 cm^{-1} are due to isocyanate species, NCO. The commencement of their formation and of the band at 1880 cm^{-1} corresponds to

(6) Ungar, R. K.; Baird, M. C. *J. Chem. Soc., Chem. Commun.* **1986**, 643.
(7) Morrow, B. A.; Ramamurthy, P. *J. Phys. Chem.* **1973**, *77*, 3052.

Table I. Observed IR Bands (cm^{-1}) due to Surface Species and Their Assignment

isocyanate (NCO)	carbonyl (CO)	nitrosyl (NO)
2272, 2222, 2200	2128, 2105, 2070, 2050	1880, ^a 1830, 1800, ^a 1795, 1700 ^a

^a Although the exact frequency is dependent upon intensity (shifts by ca. $\pm 5 \text{ cm}^{-1}$), in the text these species are referred to as the 1880/1800- and 1700- cm^{-1} species, respectively.

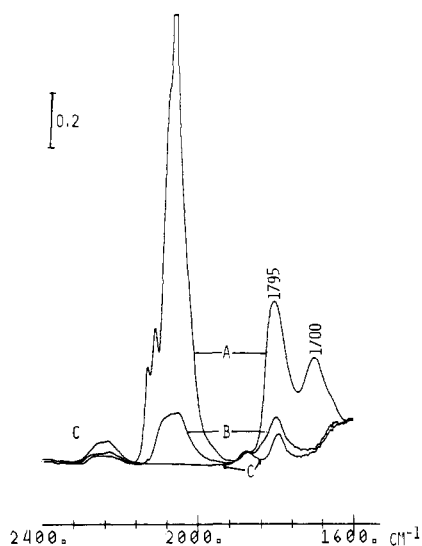


Figure 4. Coadsorption of $\text{Co}(\text{CO})_3\text{NO}$ with excess CO: (A) spectrum after 4 days of reaction (gas phase present but subtracted); (B, C) spectra after evacuation for 5 min and 12 h, respectively. The carbonyl peak in curve A has been truncated at an absorbance of 2.0.

the point, after about 4 min of adsorption, when the CO bands and the 1700- cm^{-1} band have reached their maximum intensity. We will show that associated with the 1880- cm^{-1} band is another stronger band at 1800 cm^{-1} and that the changes observed at 1800 cm^{-1} in Figure 2 are due to the growth of this band and the decrease of the 1795- cm^{-1} band. After 7 days CO was found in the gas phase.

Figure 3 shows the spectral changes that occurred following evacuation after 7 days of adsorption. The remaining CO bands and the band at 1700 cm^{-1} diminished rapidly, and after a few minutes, a new strong shoulder appeared at 1830 cm^{-1} . The difference spectrum (Figure 3D) clearly shows the evolution of these changes, where "peaks" going upward represent a decrease in intensity and those going downward show the creation of new bands. Since the major change is loss of CO and the creation of an 1830- cm^{-1} band, one might suppose that a linear CoCO species is converted to a bridged $(\text{Co})_2\text{CO}$ species. However, experiments to be described later involving ^{13}CO and ^{15}NO show that the 1830- cm^{-1} band is due to another adsorbed NO species. Finally, addition of excess gaseous NO after evacuation resulted (Figure 3C) in the immediate disappearance of the 1830- cm^{-1} band, the creation of a large 1880/1800- cm^{-1} doublet, and an increase in the NCO band at 2272 cm^{-1} at the expense of the 2222- and 2200- cm^{-1} NCO bands. No further changes occurred following prolonged evacuation or readdition of NO. The 1880/1800- cm^{-1} band intensity after addition of NO (Figure 3C) was about 2.8 times greater than it was before evacuation (Figure 3A).

The adsorption of $\text{Co}(\text{CO})_3\text{NO}$ on Al_2O_3 is complex insofar as three $\nu(\text{NCO})$, four $\nu(\text{CO})$, and five $\nu(\text{NO})$ bands have been observed. Table I lists the major bands with a simplified assignment that does not specify the nature of the metal center involved. A more detailed assignment will be discussed later.

Figure 4 shows the IR spectrum recorded following the coadsorption of $\text{Co}(\text{CO})_3\text{NO}$ with an excess of gaseous CO. In this case the sample remained yellow and even after 4 days bands due to gaseous $\text{Co}(\text{CO})_3\text{NO}$ could be detected. The CO bands are essentially unchanged relative to those in Figure 1 or 2 (but they

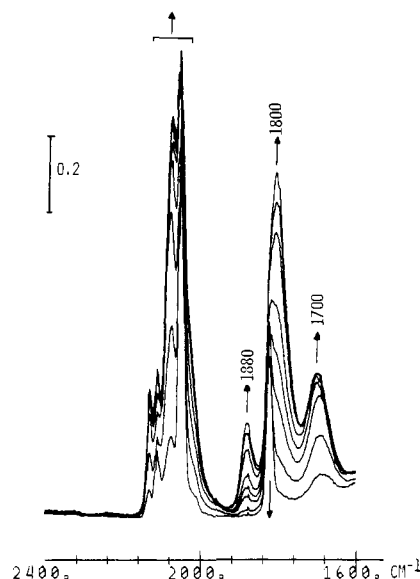


Figure 5. Spectra observed during the initial adsorption of $\text{Co}(\text{CO})_3\text{NO}$ with excess NO after 2 s, 5 s, 13 s, 21 s, 40 s, 2 min, 4 min, and 6 min. All peaks are increasing except for the sharp peak at 1817 cm^{-1} due to gaseous $\text{Co}(\text{CO})_3\text{NO}$.

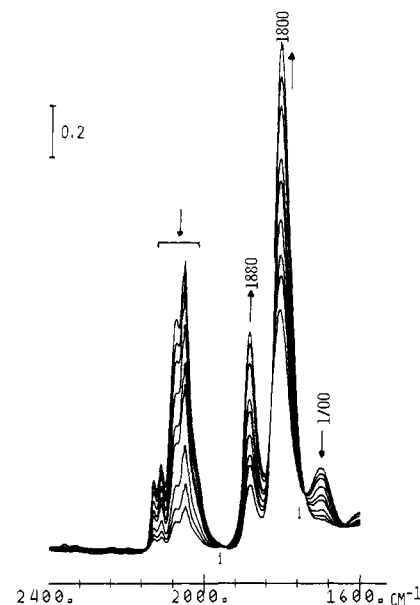


Figure 6. Continuation of Figure 5 after 9 min, 12 min, 18 min, 35 min, 70 min, 100 min, 4 h, 6 h, and 9 h. Arrows indicate the direction of intensity change.

are more intense), there is a strong pair of $\nu(\text{NO})$ bands at 1795/1700 cm^{-1} , and the formation of isocyanate and the 1880- cm^{-1} band was virtually suppressed. Evacuation rapidly removed most of the bands (Figure 4B,C), leaving a weak 1880/1800- cm^{-1} pair. Upon subsequent addition of excess NO a very weak pair of bands at 1880/1800 cm^{-1} appeared (not shown), whose intensity was about 5% of that shown in Figure 3C. This indicates that few cobalt atoms remained and implies that the 1795- and 1700- cm^{-1} species are loosely bonded to alumina in excess CO.

Figure 5 shows the spectral changes observed during the first 6 min following the coadsorption of $\text{Co}(\text{CO})_3\text{NO}$ with excess NO. In addition to the usual $\nu(\text{CO})$ bands, the $\nu(\text{NO})$ bands at 1880, 1800, and 1700 cm^{-1} continuously grow in intensity. Isocyanate formation does not occur, and there were no bands below 1600 cm^{-1} . Beyond 6 min of reaction (Figure 6) the CO bands and the 1700- cm^{-1} band start to decrease in intensity while the 1880/1800- cm^{-1} pair continue to grow. However, the ratio of the intensity of the 1800- cm^{-1} band to that of the 1880- cm^{-1} band (referred to as "R" in what follows) steadily decreased, starting

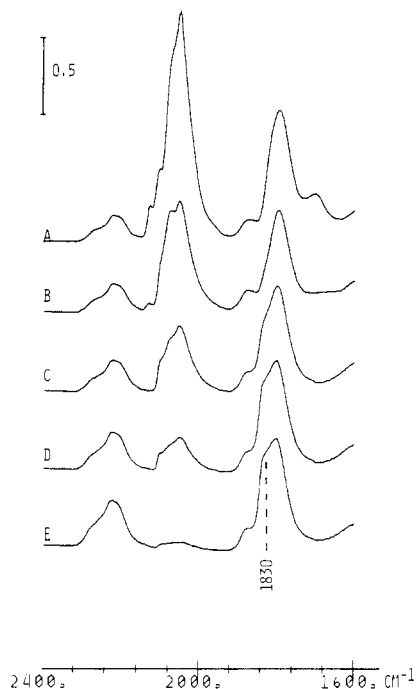


Figure 7. Deposition of $\text{Co}(\text{CO})_3\text{NO}$ on Al_2O_3 : (A) spectrum after 1 h (gas phase subtracted); (B–E) spectra after evacuation of (A) for 1 min, 5 min, 1 h, and 12 h, respectively.

at 4.0 when these bands were weakest in Figure 6 and reaching a final value of 2.2 at the end of the sequence. Most importantly, there are two clear isosbestic points at 1740 and 1950 cm^{-1} (marked "i" in Figure 6). This implies that as the 1700- cm^{-1} band and the CO bands decrease in intensity; there is a proportional increase in the intensity of the 1880/1800- cm^{-1} pair of bands. If we assume that the change near 1800 cm^{-1} are due to a decrease in the intensity of the 1795- cm^{-1} band that exactly follows the decrease in the 1700- cm^{-1} band combined with the growth of the 1880/1800- cm^{-1} pair, then the observation of a decreasing value of R as the reaction proceeds and the isosbestic points are explicable. Further, if we assume that the ratio of the intensity of the 1795- and 1700- cm^{-1} bands is as shown in Figure 4 for the coadsorption of $\text{Co}(\text{CO})_3\text{NO} + \text{CO}$, and if we subtract this contribution from the intensity at 1800 cm^{-1} in Figure 6 (based on the intensity at 1700 cm^{-1}), then the value of R is nearly constant at 2.22 during the formation of the 1880/1800- cm^{-1} bands. Therefore, we assume that the 1880/1800- cm^{-1} bands are due to a single species. However, the 1700/1795- cm^{-1} pair of bands are not due to a single species since their relative intensities varied in other experiments, but the above results show that the two species responsible for these bands nonetheless decrease in unison as the 1880/1800- cm^{-1} bands are created. Finally, a high-resolution mass spectral analysis of the gas phase showed that N_2O (but not CO_2) was present.

Figure 7 shows the spectral changes observed during evacuation after 1 h of adsorption of $\text{Co}(\text{CO})_3\text{NO}$ alone on Al_2O_3 . After 1 min of evacuation (Figure 7B) the $\nu(\text{CO})$ intensity had decreased and the 1700- cm^{-1} band was barely detectable. Evacuation for 5 min caused a further decrease in the $\nu(\text{CO})$ intensity and final removal of the 1700- cm^{-1} band and provoked the emergence of a shoulder at 1830 cm^{-1} , which steadily intensified with longer evacuation (Figure 7D,E). During the long evacuation stage, the isocyanate bands slowly intensified. Immediately after readmission of 15 Torr of CO, the $\nu(\text{CO})$ bands instantaneously reappeared (but with diminished intensity), there was a sudden growth of the NCO bands, and the 1830- cm^{-1} shoulder disappeared, accompanied by a growth of the 1800- cm^{-1} band and the reappearance of the band at 1700 cm^{-1} (Figure 8A,B). With time, the isocyanate bands continued to grow (Figure 8C).

The difference spectrum shown in Figure 9 more clearly shows the spectral changes after the addition of CO, where peaks going

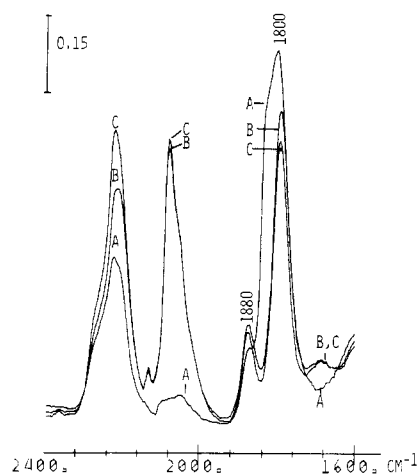


Figure 8. Deposition of $\text{Co}(\text{CO})_3\text{NO}$ on Al_2O_3 : (A) spectrum as for Figure 7D; (B) spectrum 1 min after addition of 15 Torr of CO; (C) spectrum 1 h after (B).

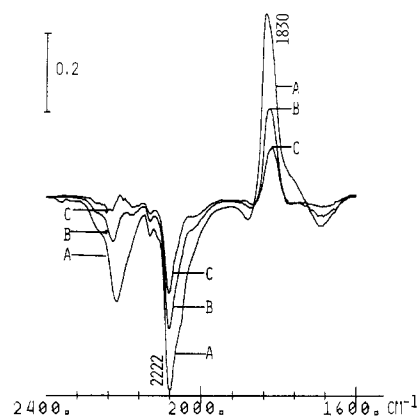


Figure 9. Difference spectra: (A) spectrum after addition of 15 Torr of CO, (A) – (C) from Figure 8; (B, C) spectra of the second and third stages of the $\pm\text{CO}$ cycle (see text), respectively.

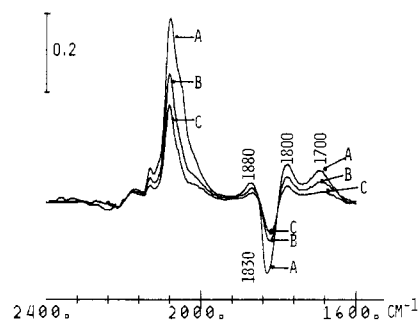


Figure 10. Difference spectra following evacuation of CO ($-\text{CO}$) in the $\pm\text{CO}$ cycle (see text): (A) spectrum C from Figure 8 (1 h under CO) minus the spectrum observed (not shown) after 1 h of evacuation; (B, C) spectra of the second and third stages of this cycle after the same reaction conditions.

upward correspond to bands that disappear and downward peaks to bands that appear. This effect was partially reversible after evacuation (Figure 10), and the cycle could be repeated three times (addition of CO, evacuation, readdition of CO, etc.) until no further changes occurred.

During this three-stage $\pm\text{CO}$ cycle (called the $\pm\text{CO}$ cycle henceforth) NCO growth continued progressively when CO(g) was present. However, the final spectrum after this cycle was similar (not shown) to that which was observed after 7 days of adsorption (Figure 3A) with respect to the NCO band intensity although the 1880/1800- cm^{-1} band intensity was about half of that shown in Figure 3A. However, after addition of excess NO, the spectrum was very similar to that shown in Figure 3C with

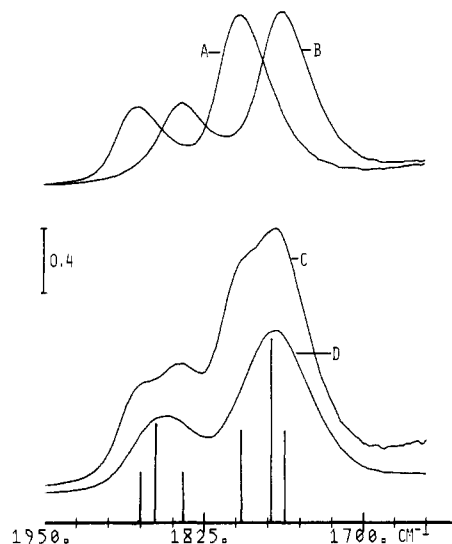


Figure 11. (A) Spectrum showing the 1880/1800- cm^{-1} bands after deposition of $\text{Co}(\text{CO})_3(^{14}\text{NO})_2$ on Al_2O_3 under conditions where only these bands are present (see text). (B) Spectrum after exposure of (A) to 15 Torr of ^{15}NO for 10 min (complete exchange). (C) Spectrum showing the sum of (A) and (B). (D) Observed spectrum after exchange with a 1:1 mixture of ^{14}NO and ^{15}NO . Vertical lines are at the observed or calculated frequencies for dinitrosyl ($(^{14}\text{NO})_2$, $^{14}\text{NO}^{15}\text{NO}$, and $(^{15}\text{NO})_2$), with intensities in the ratio 1:2:1 (see text).

respect to both the changes in the relative intensities of the NCO bands and the final 1880/1800- cm^{-1} intensity. Therefore, the final state after 7 days plus NO is very similar to that which can be generated within a few hours following adsorption of $\text{Co}(\text{CO})_3\text{NO}$, provided that one goes through three cycles of evacuation and readdition of CO.

The 1880/1800- cm^{-1} bands were very intense if excess NO was added at any stage after adsorption of $\text{Co}(\text{CO})_3\text{NO}$ (or following coadsorption with excess NO), and bands near these frequencies have generally been attributed to a cobalt combined with two NO's. Therefore, in order to confirm this assignment, as well as the other assignments, we have studied the exchange reactions by using ^{13}CO and ^{15}NO .

Although $\text{Co}(\text{CO})_3^{14}\text{NO}$ does not exchange easily with ^{15}NO in the gas phase at 20 $^\circ\text{C}$, the adsorbed species rapidly exchanged and we were able to determine that all of the observed bands from 1900 to 1700 cm^{-1} underwent the predicted shift of about 34 cm^{-1} . Similarly, the bands between 2128 and 2050 cm^{-1} shifted by about 46 cm^{-1} when ^{13}CO was used. Most significantly, during the $\pm\text{CO}$ cycle (Figures 8–10), if ^{13}CO was used, the 1830- cm^{-1} band remained at 1830 cm^{-1} whereas it shifted to 1790 cm^{-1} if the surface had been preexchanged with ^{15}NO . The NCO bands also underwent the expected shift⁸ of 60 cm^{-1} for ^{13}C substitution (we could not use ^{15}NO since, in excess NO, isocyanate formation is inhibited).

The nitrogen-15 experiments have also enabled us to establish that the 1880/1800- cm^{-1} bands were due to a species containing cobalt attached to two NO's. Figure 11 shows the ^{14}NO spectrum (A) and the ^{15}NO spectrum (B) after exchange, and it shows the sum of these two spectra (C). The last would be expected to be observed upon exchange with a 1:1 mixture of ^{14}NO and ^{15}NO if the species responsible for the 1880- and 1800- cm^{-1} bands were due to NO species on independent noninteracting sites. However, for two NO's per cobalt one would obtain a 1:2:1 mixture of $(^{14}\text{NO})_2$, $(^{14}\text{NO}^{15}\text{NO})$, and $(^{15}\text{NO})_2$. The observed spectrum in Figure 11D is very different from the sum spectrum in Figure 11C. Using standard procedures⁹ and using the observed frequencies for the $^{14}\text{N}/^{14}\text{N}$ species (1880- and 1800- cm^{-1} bands), we have calculated the expected positions for the other $^{14}\text{N}/^{15}\text{N}$ and

Table II. Calculated and Observed Frequencies (cm^{-1}) for $(\text{NO})_2$ Dimers (Figure 11)

$(^{14}\text{NO})_2$	$(^{15}\text{NO})_2$		$^{14}\text{NO}^{15}\text{NO}$
	obsd ^a	calcd	
1876	1842	1844	1863
1795	1763	1761	1774

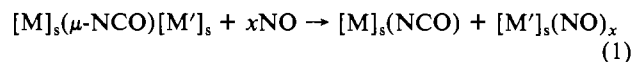
^a Values used for calculation of the force constants ($k_1 = 14.821$ $\text{mdyn } \text{Å}^{-1}$ and $k_2 = 0.672$ $\text{mdyn } \text{Å}^{-1}$, where k_2 is the interaction constant and k_1 is the NO stretching force constant) corresponding to the $\nu(\text{NO})$'s of the 1880/1800- cm^{-1} species in the presence of excess NO.

$^{15}\text{N}/^{14}\text{N}$ species (Table II), and a bar graph reconstruction is shown in Figure 11. From both the table and the reconstruction it can be seen that, given the breadth of the bands, the observed spectrum can be accounted for in spite of our failure to resolve the 1:2:1 splitting expected for each isotopic variant. Therefore, we conclude that the 1880/1880- cm^{-1} species results from the combination of a cobalt with two NO's. On the other hand, the 1830- cm^{-1} species is most likely a mononitrosyl as shown by the various difference spectra, as are also probably the 1700- and 1795- cm^{-1} species.

Discussion

The most interesting result of this work, and a priori the least expected one, is the ease with which surface isocyanates (NCO)_s can be created from NO and CO ligands at room temperature, following the deposition of $\text{Co}(\text{CO})_3(\text{NO})$ on alumina. Further, although the spectra are quite complex, the observation of several isosbestic points shortly after the initial deposition (or during deposition in excess NO) suggests that a relatively simple process is operative.

The NCO absorption band contains three maxima at 2272, 2222, and 2200 cm^{-1} , indicating the presence of more than one type of coordinated NCO ligand. In principle, these types could differ with regard to the coordination mode, with a NCO connecting to one metal or acting as a bridge between two. They could differ also by the nature and/or the oxidation state of the metals involved. Finally, the admission of excess NO at any stage of the reaction always triggered an irreversible decrease in the intensity of the two lower NCO bands with a concomitant increase of the highest one at 2272 cm^{-1} . This could result from the cleavage of μ -NCO bridges according to eq 1, the complete



$$x \geq 1$$

transfer of NCO onto one metal, the other yielding a NO complex. (In this paper, brackets will always represent a number of unspecified ligands attached to the metal and the subscript s identifies a surface species.) For example, it is well-known¹⁰ that isocyanates that are formed during the NO/CO reaction on some alumina-supported transition-metal catalysts migrate to the support, forming $\text{Al}_s^{\text{III}}\text{NCO}$ species that absorb at 2272 cm^{-1} . Therefore, the band at this frequency might be similarly assigned.

In order to discuss the other experimental results, we will first discuss the nature of the surface complexes and then we will suggest a possible reaction pathway to account for the formation of $(\text{NCO})_s$.

(1) $[\text{M}(\text{NO})_n]_x$ Type of the Surface Species Detected by IR. The $\{\text{M}(\text{NO})_n\}_x$ notation of Feltham and Enemark¹¹ has been used frequently in homogeneous coordination chemistry but rarely in surface chemistry. In a polynitrosyl complex $[\text{M}](\text{NO})_n$ of the type $\{\text{M}(\text{NO})_n\}_x$, x would be the number of metallic d electrons if all the NO ligands were considered formally as NO^+ , irrespective of their actual mode of coordination, be it linear or bent. A $[\text{M}](\text{NO})_n$ complex of this type could in principle be generated upon the complexation of the metallic fragment $[\text{M}]$, in which

(8) Morrow, B. A.; Cody, I. A. *J. Chem. Soc., Faraday Trans. 1* **1975**, *71*, 1021.
 (9) Kugler, E. L.; Gryder, J. W. *J. Catal.* **1975**, *36*, 152.

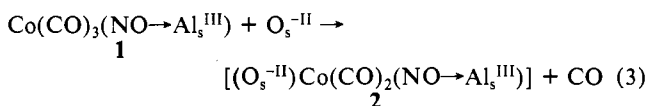
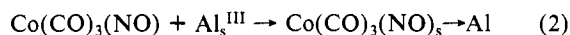
(10) (a) Solymosi, F.; Sarkany, J. *Appl. Surf. Sci.* **1979**, *3*, 68. (b) Solymosi, F.; Bansagi, T. *J. Phys. Chem.* **1979**, *83*, 552.
 (11) Enemark, J. H.; Feltham, R. D. *Coord. Chem. Rev.* **1974**, *13*, 339.

the metal M has the electronic configuration d^{x-n} , with NO gas. As an example, $\text{Co}(\text{CO})_3(\text{NO})$ is a $\{\text{MNO}\}^{10}$ complex that could then be obtained formally from the reaction of neutral NO with the metallic fragment $\text{Co}(\text{CO})_3$, in which Co is d^9 and therefore is in the zero formal oxidation state.

(a) **The 1700- and 1795- cm^{-1} Mononitrosyls.** The mononitrosyl surface species with bands at 1700 and 1795 cm^{-1} result from the direct interaction between alumina and $\text{Co}(\text{CO})_3(\text{NO})$ since they are formed initially in all cases. The coadsorption with CO has shown that these species are loosely bound to alumina in the presence of excess CO. By analogy with the deposition of metal carbonyl complexes on refractory oxides,³ these weak interactions between the support and $\text{Co}(\text{CO})_3(\text{NO})$ to yield the 1700- and 1795- cm^{-1} species are likely to be of the Lewis acid-base type. Consequently, the 1700- and 1795- cm^{-1} mononitrosyl complexes should remain $\{\text{MNO}\}^{10}$, like the parent compound $\text{Co}(\text{CO})_3(\text{NO})$. For simplicity, we will represent both of these complexes simply as $\text{Co}_s^0(\text{CO})(\text{NO})$, where it is understood there is one NO ligand and at least one CO ligand.

The structures that would be tentatively suggested for these surface species must take account of the observation that the $\nu(\text{NO})$ frequencies are lower than that of the parent compound whereas the $\nu(\text{CO})$ frequencies are not lower than those of $\text{Co}(\text{CO})_3(\text{NO})$. One of them (i.e. 2128 cm^{-1}) is even at a higher frequency (see Table I).

Alumina activated at 450 °C has Al_s^{III} Lewis acid sites and O_s^{II} donor sites.¹² Furthermore, under homogeneous conditions, examples of interactions between Lewis acids and the nitrosyl oxygen atom of NO complexes are known. This is the case in particular for $\text{Fe}(\text{CO})_3(\text{NO})^-$, isoelectronic with $\text{Co}(\text{CO})_3(\text{NO})$, or its PPh_3 substitution products.¹³⁻¹⁴ It is then conceivable that $\text{Co}(\text{CO})_3(\text{NO})$ could interact in the same manner with an Al_s^{III} site according to eq 2 (the mode of attachment has been suggested



for $\text{Co}(\text{CO})_3(\text{NO})$ on a zeolite⁶). The $\nu(\text{NO})$ and $\nu(\text{CO})$ frequencies of **1** should be lower and higher, respectively, relative to those of the parent complex.¹⁵ Complex **1** could react further with a O_s^{II} donor site in a proper location to yield the substitution product **2** according to eq 3. Its $\nu(\text{NO})$ must be lower than that of **1**, and **2** could be then the 1700- cm^{-1} species, while **1** becomes the 1795- cm^{-1} one. The $\nu(\text{CO})$ frequencies of **2** should also be lower than those of **1**, but their location relative to those of $\text{Co}(\text{CO})_3(\text{NO})$ is difficult to assess without knowing the strength of the $\text{O}_s^{\text{II}} \rightarrow \text{Co}$ interaction. It must be emphasized that formulations other than **1** and **2** are equally compatible with the IR data.

Formulations of the 1700- cm^{-1} species with a bent NO cannot be rejected a priori. However, in the formulation **2** presented, we believe that the types of interactions considered suffices to rationalize the $\nu(\text{NO})$ band at 1700 cm^{-1} with the NO still linearly bound to cobalt. Formulations such as $\text{O}^{\text{II}} \rightarrow \text{Co}(\text{CO})_2(\text{NO})$ or $(\text{O}_s^{\text{II}})^+ \text{---CO---Co}(\text{CO})_2(\text{NO})$ implicating solely a surface donor site can probably be dismissed for both the $\nu(\text{CO})$'s, and $\nu(\text{NO})$ should be expected at lower frequencies than in $\text{Co}(\text{CO})_3(\text{NO})$.

Whatever the exact formulation of the 1700- and 1795- cm^{-1} species, the important point is that we assume that they result

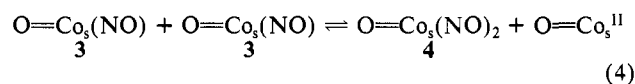
from Lewis acid-base interactions between alumina and $\text{Co}(\text{CO})_3(\text{NO})$. Consequently, they remain, like $\text{Co}(\text{CO})_3(\text{NO})$, $\{\text{MNO}\}^{10}$. Simple decomplexation of neutral NO would leave $\text{Co}_s^0(\text{CO})$ sites with the cobalt in the 0 oxidation state.

(b) **The 1880/1800- cm^{-1} Dinitrosyl and the 1830- cm^{-1} Mononitrosyl Species.** NO adsorbed on various solid supports containing cobalt such as Co^{II}-exchanged X and Y zeolites,^{16,17} cobalt oxides,^{1a} and the cobalt spinel CoAl_2O_4 ^{1a} invariably shows a pair of prominent bands at 1860–1910 and 1780–1800 cm^{-1} with the one at lower frequency being the strongest by a factor of 2.0:4.5. These bands have been assigned to a *dinitrosyl* resulting from the complexation of NO onto Co^{II}. Therefore, the species with $\nu(\text{NO})$ bands at 1880 and 1800 cm^{-1} observed in this work is also probably a dinitrosyl of the $\{\text{M}(\text{NO})_2\}^9$ type. Simple removal of neutral NO would then leave cobalt in the II oxidation state.

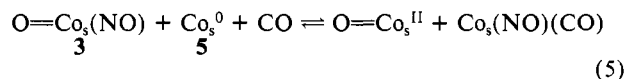
For each $(\text{NCO})_s$ formed from NO and CO, an oxygen has to be transferred to another atom, which becomes oxidized. Although during $(\text{NCO})_s$ formation low-frequency bands (below 1600 cm^{-1}) appear, which might be assigned to surface nitrites, nitrates, and/or carbonates, their intensity is weak, and we do not believe that they could account for most of the oxygen released. Further, these bands were virtually nonexistent during the $\pm\text{CO}$ cycle. Therefore, cobalt is the most likely oxygen acceptor. On that basis, we will formulate arbitrarily the 1880/1800- cm^{-1} species as $\text{O}=\text{Co}_s(\text{NO})_2$, recognizing however that an ionic $\text{O}^{2-} \cdots \text{Co}_s^{2+}$ interaction could be equally possible.

For simplicity, the cobalt sites on which the 1880/1800- cm^{-1} dinitrosyl and the 1700- and 1795- cm^{-1} mononitrosyls are elaborated will be identified as oxidized and reduced sites, respectively. In the denitrosylated form, they will be further labeled as bare sites. During evacuation, before excess NO is added, the 1880/1800- cm^{-1} dinitrosyl is easily converted to a mononitrosyl having $\nu(\text{NO})$ at 1830 cm^{-1} (Figures 3B,D and 7). From the $\pm\text{CO}$ cycle, we know that this species is unstable under CO (Figures 8 and 9) and it is therefore likely devoid of CO ligands. Upon admission of CO, the 1830- cm^{-1} species yields the 1880/1800- cm^{-1} dinitrosyl and the 1700- cm^{-1} mononitrosyl (Figure 10), although in decreasing amounts as the number of cycles increases. We will assume that excess CO simply induces a redistribution of the NO ligands, leaving a constant number of oxidized and reduced sites. The 1830- cm^{-1} species can then be a NO on an oxidized site, a $\{\text{MNO}\}^8$ type as for example $\text{O}=\text{Co}(\text{NO})$, or a NO on a reduced site, a $\{\text{MNO}\}^{10}$ type such as $\text{Co}(\text{NO})$, with no CO ligand in both cases. The formulation $\text{Co}(\text{NO})$ can be easily rejected, for the hypothetical highly coordinatively unsaturated binary compound $\text{Co}(\text{NO})$ should behave as an acceptor toward the donor sites of the surface and its $\nu(\text{NO})$ should be below that of $\text{Co}(\text{CO})_3(\text{NO})$ at 1817 cm^{-1} , not above. That the observed frequency at 1830 cm^{-1} is almost midway between those of the 1880/1800- cm^{-1} dinitrosyl is however fully consistent with a formulation such as $\text{O}=\text{Co}_s(\text{NO})$. It is of interest to note that a mononitrosyl with $\nu(\text{NO})$ at 1870 cm^{-1} has been reported in the reaction of gaseous NO with Co^{II}-zeolite A.¹⁶

The interconvertibility of the 1830- and 1880/1800- cm^{-1} species **3** and **4** could then be accounted for according to the NO-exchange reaction eq 4. We have to postulate that, in the presence of CO,

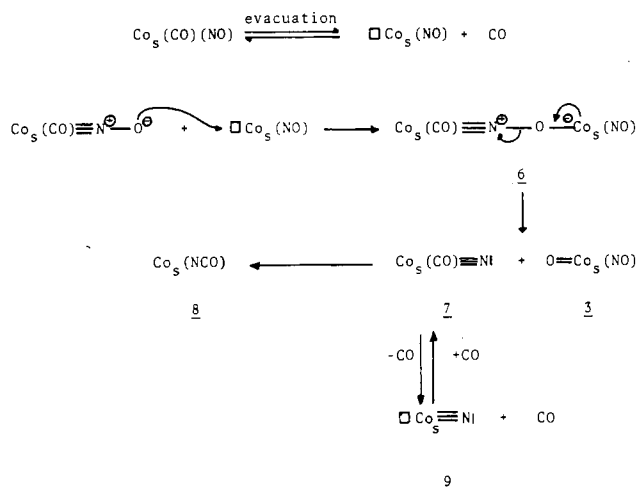


carbonylation of the bare oxidized sites $\text{O}=\text{Co}_s^{\text{II}}$ would shift the equilibrium strongly in favor of **4** to account for the observations. In a similar manner, migration of NO to a bare reduced site Co_s^0 (**5**) would regenerate the 1700- cm^{-1} species according to eq 5,



- (12) Knözinger, H.; Ratnasamy, P. *Catal. Rev.* **1978**, *17*, 31.
 (13) Pannell, K. H.; Chen, Y.; Belknap, K.; Wu, C. C.; Bernal, I.; Creswick, M. W.; Hsu Nan Huang *Inorg. Chem.* **1983**, *22*, 418.
 (14) Roustan, J. L.; Forgues, A.; Merour, J. Y.; Venayak, N. D.; Morrow, B. A. *Can. J. Chem.* **1983**, *61*, 1339.
 (15) For the expected directions of shift in the $\nu(\text{NO})$'s and $\nu(\text{CO})$'s upon complexation of a Lewis acid on either the metal or the O atom of a CO or a NO ligand in mixed-NO/CO complexes see for example: Lokshin, B. V.; Rusach, E. B.; Kolobova, N. E.; Makarov, Yu. V.; Ustynuk, N. A.; Zdanovich, V. I.; Zhakaeva, Z. Zh.; Setkina, V. N. *J. Organomet. Chem.* **1978**, *108*, 353.

- (16) Lunsford, J. H.; Hutta, P. J.; Lin, M. J.; Windhorst, K. A. *Inorg. Chem.* **1978**, *17*, 606.
 (17) Pralaid, H.; Coudurier, G. F.; Ben Taarit, Y. *J. Chem. Soc., Faraday Trans. 1* **1978**, *74*, 3000.

Scheme I^a

^aThe symbol \square represents explicitly an unoccupied coordination site. Only one canonical form is shown for the $\text{Co}_s(\text{NO})$ bond.

provided that such sites are present on the surface. We will show in the next section how the results pertaining to the formation of $(\text{NCO})_s$ can be used to indicate possible modes of formation of bare Co_s^0 (**5**).

(2) **Formation of Surface Isocyanates $(\text{NCO})_s$.** In order to devise a reaction pathway compatible with the experimental observations, we must take account of the following: (1) the inhibiting effect of excess CO on the formation of $(\text{NCO})_s$, (2) the observation that the formation of $(\text{NCO})_s$ was more rapid in the $\pm\text{CO}$ cycle and the need to have more than one cycle in order to bring the reactions to completion, and (3) in the $\pm\text{CO}$ cycle, the sudden growth of $(\text{NCO})_s$ right after the admission of CO at the end of each cycle, followed by a slower growth under CO, the latter regime being particularly significant in the first cycle.

We will show that the simplest model that accounts for these observations is one in which we assume that surface nitrides are formed. We will first discuss the formation of $(\text{NCO})_s$ under static conditions and expand on the model in light of the observations pertaining to the $\pm\text{CO}$ cycle.

In this model presented in Scheme I, we propose that one of the initially absorbed $\text{Co}_s(\text{CO})(\text{NO})$ complexes undergoes a decarbonylation and can then play the role of the oxygen acceptor from the nitrosyl of an adjacent $\text{Co}_s(\text{CO})(\text{NO})$. The transient bimetallic species **6** thus formed fragments into the nitride **7** and the 1830-cm^{-1} mononitrosyl **3**. When CO gas is present, **3** is unstable and converts to $\text{O}=\text{Co}(\text{NO})_2$ (**4**) according to eq 4.

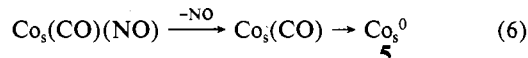
The fact that isosteric points were observed during this reaction (and also during the formation of $\text{O}=\text{Co}(\text{NO})_2$ and N_2O during the coadsorption with excess NO) suggests that the species responsible for the 1700- and 1795-cm^{-1} bands act in concert to generate $(\text{NCO})_s$ (or N_2O). Since on alumina activated at 450°C there are nearly adjacent Al_s^{III} and O_s^{II} donor sites due to elimination of H_2O , the creation of the bimetallic intermediate **6** would nicely account for the observations.

The nitride **7** goes ultimately to isocyanate **8**. Under vacuum, in the $\pm\text{CO}$ cycle, complete decarbonylation may occur at any stage up to and including the formation of **7**, in which case the CO-free nitride **9** will be generated. When CO is readded, **9** is carbonylated back into **7** to yield isocyanate **8**, and the rate of this process may be fast or slow, depending on whether the correct conditions are available for carbonylation of **9** or for the reaction between CO and the nitrido ligand.

In this scheme, excess CO has an inhibitory effect on $(\text{NCO})_s$ formation by preventing the generation of the coordinatively unsaturated and transient key intermediate $\text{Co}_s(\text{NO})$, which is required in the O-transfer step. Under vacuum, however, ligand dissociation is accelerated and the evolution of the surface is faster than under static conditions. Furthermore, under static conditions, the CO released in the gas phase, while $(\text{NCO})_s$ formation pro-

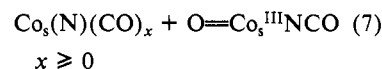
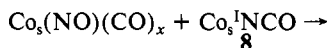
ceeds, should have a retarding effect on the production of the unsaturated intermediate.

Scheme I could also be possible if loss of NO occurs instead of CO to yield the subcarbonyl species $\text{Co}_s(\text{CO})$ and eventually reduced bare sites **5** following further loss of CO according to eq 6. However, loss of NO would also be expected to occur in the



presence of excess CO. Even after 4 days during the coadsorption experiment with CO, the 1700- and 1795-cm^{-1} species were still present with no sign of significant decomposition. Therefore, we reject eq 6 as a major route for the formation of isocyanates under static conditions. But as discussed now, eq 6 might be significant in the $\pm\text{CO}$ cycle.

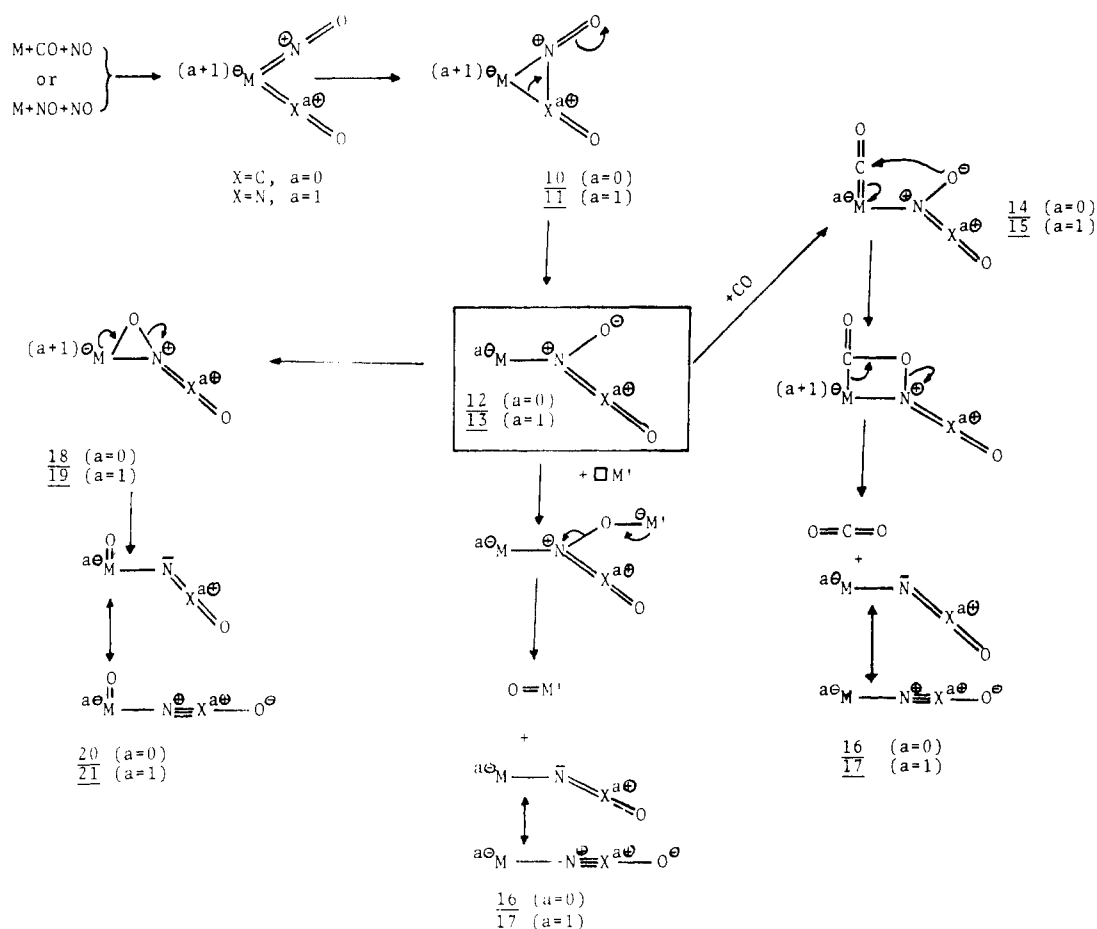
When considering Scheme I only to rationalize the results of the $\pm\text{CO}$ cycle, we would expect that evacuation followed by the admission of CO *once* should be sufficient to use all the surface NO's which can be converted into $(\text{NCO})_s$. This is evidently not the case, for more than one cycle is needed. If eq 6 comes into play, this observation is easily interpreted. Under vacuum, the reactions yielding $(\text{NCO})_s$ will stop when no more NO on reduced sites will be available, either because they have reacted according to Scheme I or because they have been irreversibly eliminated according to eq 6. The latter is expected to produce bare reduced sites Co_s^0 (**5**) under dynamic vacuum. At that point, all the remaining NO's will be on oxidized sites and they are no longer reactive. However, upon admission of excess CO, part of these NO's can migrate back to the bare reduced sites **5** to re-form the 1700-cm^{-1} species according to eq 5. At the beginning of the next cycle, during the evacuation step, they can therefore reenter the $(\text{NCO})_s$ -forming route of Scheme I and the same process is repeated again until there are no more reduced sites, which signals the completion of the reactions. Evidently, once formed, the bare reduced sites Co_s^0 could also serve as oxygen acceptors, as well as the isocyanates **8**, which could be converted into isocyanato- Co^{III} complexes according to eq 7. In addition, bare oxidized sites could



also participate in the formation of NCO-bridged bimetallic species. It might therefore be not surprising that several $\nu(\text{NCO})$ bands were observed.

(3) **Alternate Reaction Pathways for $(\text{NCO})_s$ Formation.** In the nitride route exemplified by Scheme I, cleavage of the N-O bond precedes the formation of the N-C bond. Alternatives in which N-C bond formation occurs *first* can be envisioned also. For example, a *coupling* reaction between a NO and a CO attached to the same metal has been suggested as an initial step in the formation of $\text{Cp}_2\text{Ti}(\text{NCO})$ from $\text{Cp}_2\text{Ti}(\text{CO})_2 + \text{NO}$ under homogeneous conditions.¹⁸ Accordingly, Scheme II could have been considered as well with $X = \text{C}$ and $a = 0$ applying for the formation of $(\text{NCO})_s$. In Scheme II excess CO could block the O-transfer step (as in the nitride route) but should not prevent the formation of **10**, for the metal coordination number remains constant. Moreover, carbonylation of **12** could yield the more stable coordinatively saturated derivative **14**. As already pointed out, after 4 days under CO, the ubiquitous 1700- and 1795-cm^{-1} species were still present with only a very weak absorption in the $\nu(\text{NCO})$ region. To retain Scheme II as a plausible major reaction route toward $(\text{NCO})_s$, it should be further assumed that, even under CO, the steps leading to **10**, **12**, and **14** are reversible and strongly displaced toward $\text{M}(\text{CO})(\text{NO})$ ($\text{M} = \text{Co}_s$, $a = 0$, $X = \text{C}$). Furthermore, Scheme II fails to rationalize in a simple way the fast formation of $(\text{NCO})_s$ in the $\pm\text{CO}$ cycle immediately after the admission of CO. The nitride route exemplified by Scheme I is indeed the simplest hypothesis for accounting for most of the observations.

Scheme II



We cannot dismiss however the possibility that, under static conditions, when the surface is slowly evolving, a small amount of $(NCO)_3$ could be formed according to Scheme II. An oxygen transfer implicating **14** to yield **16** + CO_2 would account nicely for the formation of a small amount of surface carbonates.¹⁹

(4) Reactions under Excess NO. During the coadsorption of $Co(CO)_3(NO)$ with excess NO, the 1880/1800- cm^{-1} dinitrosyl started to form within seconds of adsorption, indicating a rapid oxidation of the surface, and N_2O was evolved into the gas phase. The unsaturated species required at the start of the sequence of Scheme I could react with excess NO to yield dinitrosyl species on reduced sites, which could create a new situation relative to the one pertaining to the formation of $(NCO)_3$. In consequence, the nitride route we have retained previously for the reasons indicated does not necessarily apply to the reactions with excess NO.

Schemes I and II are applicable for the formation of N_2O and $O=Co(NO)_2$. All that is required in Scheme I is a NO for CO substitution to yield a nitrosylated nitride rather than a carbonylated one. Scheme II applies as such with $X = N$ and $a = 1$. In both cases one obtains ultimately a N-bonded N_2O complex rather than a $M-NCO$ species, with subsequent evolution of N_2O into the gas phase.

Interestingly, Scheme II with $X = N$ and $a = 1$ yielding ultimately **17** + CO_2 provides an explicit plausible sequence of bond-forming and bond-breaking steps for the $2NO + CO \rightarrow N_2O + CO_2$ reaction catalyzed by complexes such as $M(NO)_2(PPh_3)_2^{+20}$ ($M = Rh, Ir$). But, as in the conditions under which

$(NCO)_3$ were formed, Co remaining the predominant O acceptor, such a route would at best play a minor role in the present case. Finally, we point out that the presence of isosbestic points during the reactions under excess NO has suggested that the 1700- and 1795- cm^{-1} species could be involved in a synchronous manner. Therefore, during that period when such a situation prevails, an O-transfer step implicating only one metal center as from **13** to **21** can also be dismissed.

Conclusion

The high vapor pressure of $Co(CO)_3(NO)$ at room temperature makes the deposition of the compound a trivial operation compared to the techniques of sublimation or impregnation in solution. Seemingly volatile nitrosyl complexes of other metals might then be useful for depositing the metallic element already in a low oxidation state. However, in the absence of excess CO, the results reported point to the occurrence of a facile reaction at room temperature resulting in the oxidation of the metal with the concomitant formation of surface isocyanates. The latter reaction might even prove to be typical of deposited mixed carbonyl-nitrosyl metal complexes. Studies with other NO-CO complexes are aimed to address this question as well as to obtain additional information in favor of or against the nitride route considered here. Our results relative to the interactions of the dinitrosyl iron complex $Fe(CO)_2(NO)_2$ with alumina to be reported later on have indeed shown that $(NCO)_3$ formation is equally facile at room temperature and is also strongly inhibited by an excess of CO.

Acknowledgment. We wish to thank the Natural Sciences and Engineering Research Council of Canada for financial support.

Registry No. **1**, 14096-82-3; **4**, 108693-56-7; Al_2O_3 , 1344-28-1; CO, 630-08-0; NO, 10102-43-9; N_2O , 10024-97-2.

(19) Intermediates **12** and **13** in Scheme II are analogous to N-bonded nitrito complexes. In each case there is an sp^3 tetravalent N atom singly bonded to both the metal and a negatively charged (i.e. nucleophilic) oxygen atom. Furthermore, in the reaction pathway **12/13** \rightarrow **16/17** + CO_2 with CO as the oxygen acceptor, the metallacycle shown with $X = C$ and $a = 0$ is analogous to an explicit VB representation of the metallacycle depicted in ref 21 relative to the nitrosylation reaction of $Fe(CO)_5$ with NO_2^- to yield $Fe(CO)_5(NO)^-$.

(20) Bhaduri, S.; Johnson, B. F. G. *Transition Met. Chem. (Weinheim, Ger.)* **1978**, *3*, 156.

(21) Stevens, R. E.; Gladfelter, W. L. *Inorg. Chem.* **1983**, *22*, 2034.